Environmental Science and Pollution Research (2019) 26:13702–13716
https://doi.org/10.1007/s11356-018-2096-x

SUSTAINABLE ENVIRONMENTAL MANAGEMENT

Total sediment transport from an urbanizing watershed in the upper Yellow River, China

Zhijun Wang [1,2,3] · Wanquan Ta [2] · Jian Zheng [1] · Ke Zhang [1]

Received: 5 March 2018 / Accepted: 20 April 2018 / Published online: 25 May 2018

Abstract

For many event-based, high-sediment yield rivers draining arid zones, where erosion activities in the watershed and fluvial erosion in the stream channel are nearly equally important in sediment transport, determination of fluvial sediment dynamics are of great importance in establishing reliable strategies to manage environmental changes in watershed scale. Wash load rating curve indicating watershed characteristic changes and Ackers and White's bed load function (wash load excluded) used for determining bed load transport dynamics are distinguished for the first time to recognize the true sediment transport mode in the lower Huangshui River, which is the largest tributary of the upper Yellow River, contributing a lot to the wash load of the Inner Mongolia desert reach of the Yellow River and causing complicated water-sediment response. Based on the continuous and detailed hydrological data monitored at the Minhe gauge station, our results indicated that the sediment transport regime has altered since the 1980s in response to the eco-environmental changes mainly due to urbanization, with suspended sediment concentration (SSC) decreased by 50% on average compared with the natural state (1950–1980). The combined use of wash load rating curve and theoretical bed load function derived an estimate of total sediment transport due to comprehensive ecological management since the 2000s to be 3.43 × 107 t for the lower Huangshui River, among which the total bed load is 1.40 × 107 t, and the wash load is 2.03 × 107 t. The transport ratio of wash load to total bed load is 1.45:1.

Keywords Sediment rating curve · Wash load · Bed material load · Sediment transport dynamics · Huangshui River · Yellow River

Introduction

Fluvial sediment transport is a complex process, of which the mechanisms and the related variations of sediment concentrations under different governing conditions provide insights into the evaluation of terrestrial material transport, landscape denudation, geomorphic changes, water quality, and even the ecology of downstream estuaries. Therefore, fluvial sediment dynamics is of great importance in establishing reliable strategies to manage environmental changes in watershed scale. Despite of great improvement in theoretical research through centuries by both hydraulic engineers and geologists, the understanding of fluvial sediment transport dynamics remains limited mainly due to the confusion of the true hydraulic transport modes and the lack of detailed water-sediment data to validate the representative theories in natural rivers.

From the perspective of hydraulic response, the total sediment load of a river is composed of suspended load and bed load, of which the finest part of the suspended load is wash load maintained in suspension for a long distance in the main stream of the river without deposition, and the coarse-grained components is bed load saltating and rolling on the bed. Nevertheless, a small fraction of sand to grain sediment components is also active under turbulent flow conditions and moves downstream either as bed load or as suspended

Responsible editor: Philippe Garrigues

✉ Zhijun Wang
wzj1159@163.com

[1] College of Energy and Power Engineering, Lanzhou University of Technology, 287 Langongping Road, Lanzhou, Gansu Province, China

[2] Key Laboratory of Desert and Desertification, Northwest Institute of Eco-Environment and Resources, Chinese Academy of Sciences, 320 Donggang West Road, Lanzhou, Gansu Province, China

[3] University of Chinese Academy of Sciences, 19 Yuquan Road, Beijing, China

material constantly exchanging with the bed, named as bed material load. In larger channel and even watershed scale, these different sediment components are proven to be different source-dependent or flow condition-dependent and should be treated separately.

The suspended load of a river is related to the sources and supply conditions at the watershed scale. Climate trends, vegetative cover, rainfall intensity, topographic relief, landscape processes, and human disturbances all influence the sediment yield and transport rate (Milliman and Meade 1983; Milliman and Syvitsky 1992; Trimble 1997; Dinehart 1998; Wang et al. 1998, 2016; Trimble 1999; Yang et al. 2005; Meade et al. 2010; Burbank and Anderson 2013; Ta et al. 2015; Wang et al. 2016). Thus, the suspended load appears to be an integration of the river basin characteristics above the measurement site. As the majority of suspended load, i.e., wash load is transported below theoretical transport capacities and is comparatively easy to measure but difficult to predict using stream power-related sediment transport models (Syvitski et al. 2000; Warrick and Rubin 2007), site-specific empirical relationships between river flow discharge (FD) and suspended sediment concentration (SSC), such as rating curves, are often applied, among which the simple suspended sediment rating curve commonly takes the form of a power function:

$$C = aQ^b \tag{1}$$

where C is SSC (kg m^{-3}), Q is FD (m^3 s^{-1}), and a and b are the sediment rating coefficient and exponent, respectively. Equation (1) covers both the effect of sediment availability and the erosive power of the river to transport this weathered material throughout a watershed (Asselman 2000). Thus, it is often applied for general use. However, the empirical relationships between FD and SSC may be influenced by many other factors, such as sediment yield variabilities of river tributaries (Lenzi and Marchi 2000; Murray et al. 2000; Meade et al. 2010), changes in bed sediment grain size (Rubin and Topping 2001), flow dynamics and event hysteresis (Walling 1974; Williams 1989; Rubin and Topping 2001), and seasonal to interannual changes in sediment supply (Leopold 1968; Topping et al. 2000). In addition, classical suspended sediment rating curve do not differentiate between wash load and suspended bed material, thus, the application of Eq. (1) may result in several problems regarding to the accuracy of the fitted curve and may lead to ambiguous results.

The transport rate of bed load in rivers is related to many variables, such as FD, average flow velocity, water depth, energy slope, shear stress, stream power, bed configuration, channel pattern, turbulence intensity, particle size, and water temperature (Yang 1977). Based on considerations about simplicity for application and theoretical hypothesis, several classical sediment transport theories have been put forward, such as shear stress approach (Shields 1936; Einstein 1950), regime theory (Blench 1969), velocity approach (Colby 1964), discharge approach (Meyer-Peter et al. 1934), slope approach (Meyer-Peter and Müller 1948), stochastic approach (Einstein 1950; Bishop et al. 1965), regression approach (Shen and Hung 1972), and stream power or unit stream power approach (Ackers and White 1973; Yang 1973; Yang and Francisco 2005). Each of these methods has its merits but all have limitations when used to estimate total sediment transport in natural rivers due to their complexity in application and accuracy and the difficulties in measuring the dominant variables they employed.

The Huangshui River, which is one tributary of the upper Yellow River, drains an arid and semiarid landscape that has been subjected to periodic extensive population and urban growth, as well as channel modifications, including hydropower structures. In addition, the Huangshui River is highly event driven, yielding the majority of long-term discharge and sediment transport during intensive summer flood events. Based on the multi-decadal period of climate and land-use change, the Ministry of Water Resources of the People's Republic of China continued stream gauging and daily suspended sediment sampling operations at a station near the river mouth. These measured data are exceptionally valuable. They give us the opportunity not only to evaluate the variability of water-sediment characteristic responses to eco-environmental changes, but also to determine the sediment transport dynamics based on the detailed monitored hydrological data.

Study area

Originating in the upstream Qilian Mountains, the Huangshui River is the largest tributary to the upstream reaches of the Yellow River, with a drainage area of 17,733 km^2 and a stream channel length of 374 km. It ultimately merges into the Yellow River near the Lanzhou gauge station (Fig. 1). The Huangshui River basin (Fig. 2), with a drainage area of 32,863 km^2, is a transitional region between the Tibetan Plateau and the Chinese Loess Plateau. Thus, it is characterized by widespread gullies and considerable topographic relief. The Huangshui River flows across the gullies and drains a steep inland mountainous area with lush vegetation upstream of the Xining gauge station border (Fig. 1). It also drains lower mountains and a flat inland plain in the lower watershed, where the gullies are mainly composed of highly weathered loess materials, with the surface covered with sparse vegetation. The area between the Xining and Minhe

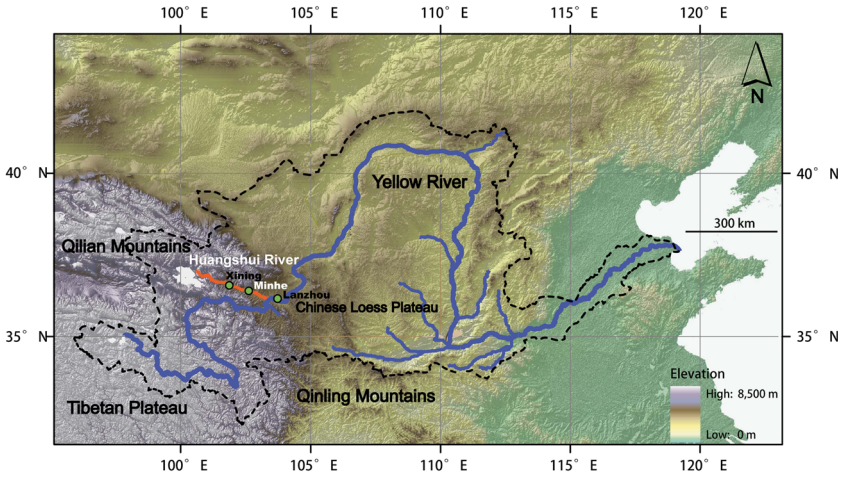

Fig. 1 Map showing the Huangshui River and the upper Yellow River. The orange line is the Huangshui River. The green dots with black borders are gauge stations. The drainage area of the Yellow River is highlighted by the thick, black, dashed contour

gauge stations has been converted into industrial and agricultural riparian areas and developed as an irrigation district in Qinghai Province, China since the 1980s, with many hydropower structures built and coming into operation. The temperature in this area has increased and the related precipitation has decreased since the 1990s (Dai et al. 2006). Comprehensive ecological management has occurred since 2000 (Wang and Tang 2012).

The lower reach of the Huangshui River is characterized by the semiarid continental climate of the plateau. The mean annual precipitation is 460.2 mm and the mean annual temperature is 5.7 °C. As the important output control gauging station on the lower Huangshui River, the Minhe gauge station is located at 102° 48′ E and 36° 20′ N and is 74 km from the river confluence (Fig. 1). Established in 1940 by the Ministry of Water Resources of the People's Republic of China, the Minhe gauge station has a drainage area of 15,342 km^2. The maximum measured FD is 1300 m^3 s^{-1} (occurring on 27 July 1952), and the maximum measured SSC was 843 kg m^{-3} (occurring on 23 July 1974). The majority of long-term suspended sediment is derived from the gullies with sparse vegetation and highly weathered loess materials within 50 km upstream of the station during summer rainfall-induced floods. The mean annual FD is 50.8 m^3 s^{-1}, and the mean annual SSC is 3.8 kg m^{-3}. The annual average suspended sediment load at the Minhe station is (1.84~2.4) × 10^7 t (Li and Quan 2011).

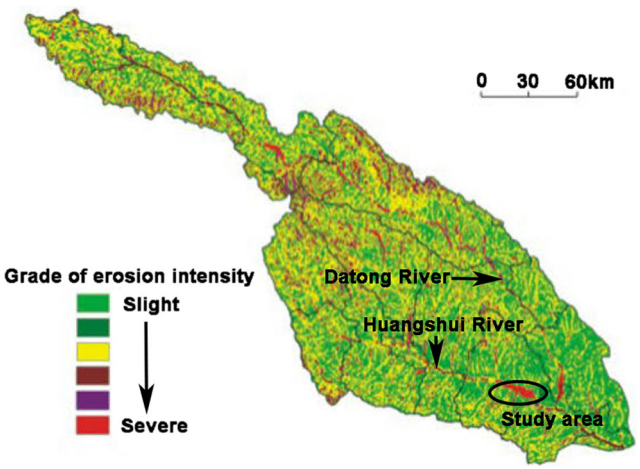

Fig. 2 Plan view of the Huangshui River basin showing different land-use types (Bai and Yan 2013)

The monthly precipitation distribution (Fig. 3a) and annual hydrographs of mean daily FD for above average (Fig. 3b), below average (Fig. 3c) and average (Fig. 3d) annual FD were plotted together with the related SSC. As shown in Fig. 3, water and sediment discharge at the Minhe gauge station on the lower Huangshui River is dominated by runoff events during the wet summer season, which mainly occurs mostly from April to October. The subsequent hydrographs exhibit rapid rises and falls, with the occurrence of SSC peaks coinciding with FD peaks. On average, approximately 78% of the annual discharge and 99.3% of the suspended sediment load occurs from April–October. These discharge patterns are representative of the event-based discharge patterns.

Because the lower Huangshui River contributes to the majority of the suspended sediment load throughout the watershed due to sparse vegetation and severe soil erosion of riparian gully-dissected slopes due to intensive summer rainfall, it serves as a unique example of a high sediment yield, mountainous river with considerable human modification. Therefore, we choose the Minhe gauge station, which has decades of continuous FD and SSC data, as the representative station in our study.

Data and methods

Daily FDs and SSCs, which were average cross-section values at the Minhe gauge station, have been measured and

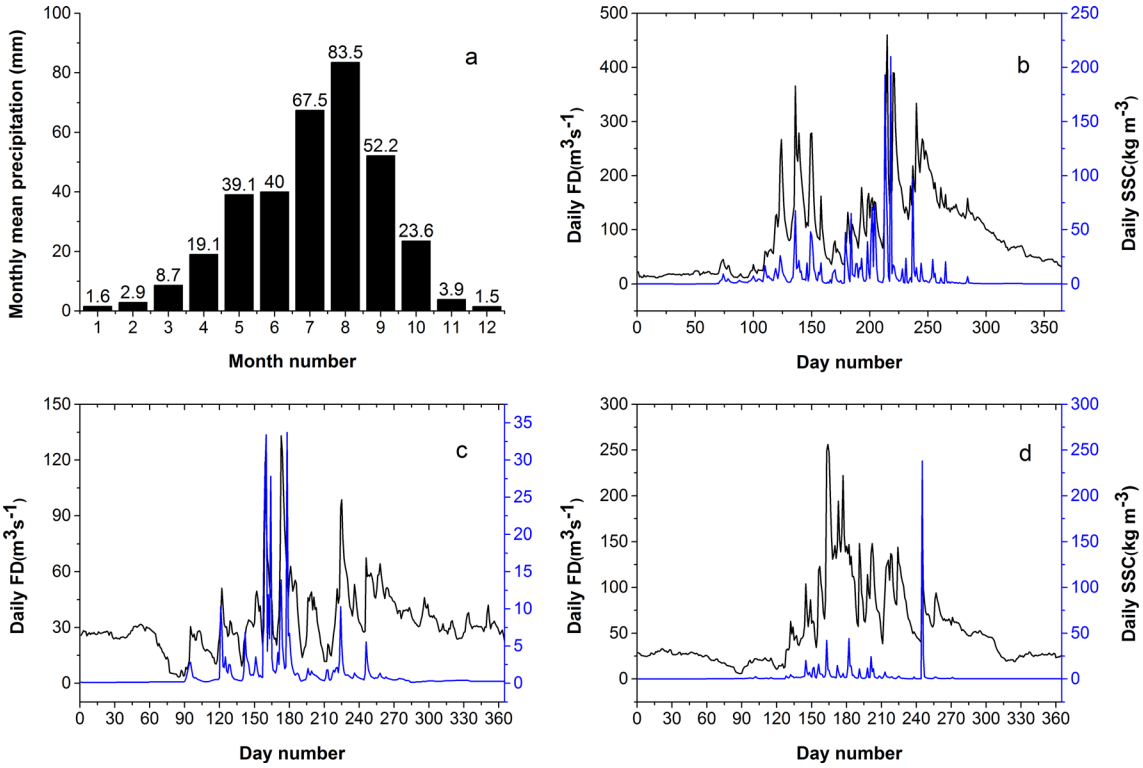

Fig. 3 Typical annual hydrographs and SSC response to monthly precipitation distribution in the lower Huangshui River. **a** Monthly precipitation distribution for **b** a high annual FD (90.69 $m^3\ s^{-1}$), 1967, **c** a low annual FD (32.38 $m^3\ s^{-1}$), 2002, and (**d**) an average annual FD (51.54 $m^3\ s^{-1}$), 1987. Blue lines represent SSC

calculated following the criteria of GB 50179-93 and GB 50179-92, respectively, which were issued by the Ministry of Water Resources of the People's Republic of China. The data from 1940 to 1949 were excluded due to lack of continuity, and the data from 2007 to 2009 were unavailable in the data series due to the shift of the gauge station to a new location 1.22 km in the upstream direction during this period. Thus, we used the 63-year continuous data from 1950 to 2015 to establish the rating relationships between SSC and FD.

According to the variability of watershed characteristics of the lower Huangshui River due to natural and man-made factors and the matching of annual FDs and SSCs, we subdivided the long-term water and sediment record into four phases: a NS period (natural state, 1950–1980), COR period (construction and operation of the reservoirs, 1980–1990), CHI period (climate and human activities interaction, 1990–2000), and SWC period (soil and water conservation, 2000–2015) (Fig. 4). Because sediment rating curves should be based on a wide range of discharges, including a sufficient number of measurements of high discharges (Asselman 2000), i.e., rating curves should be fitted based on relatively wet periods, relatively wet periods with discharges exceeding the long-term mean discharge with respect to the four periods were selected, as shown in Appendix Table 1. Correspondingly, 14 selected sediment-laden flows together with the hydrographs from 1980 to 2015 were plotted, as shown in Fig. 5. These hydrographs included several rising and falling stages. Values of peak FD and peak SSC that were too low to be identified were excluded.

In addition, the detailed instantaneous data of FD, average flow velocity, water depth, point-integrated, and cross-section averaged grain size distributions (GSDs) of suspended sediment as well as water temperature from 2010 to 2015 were also monitored and available for use. The sampling work was based on the criteria of GBT 50159-92, with samples collected at 60 cm deep under the water surface when the water depth is below 0.75 m and collected at 20, 60, and 80 cm below the water surface when the water depth exceeds 0.75 m for a depth-integrated value. The data can be used to determine the bed load dynamics.

As mentioned above, theoretical bed load transport functions have been derived taking into account of various dominant hydraulic flow factors. Here, for the Huangshui River, which is in apparent equilibrium with the bed material and the bed material load is an equilibrium capacity load (Li and Quan 2011), whose transport rate under different flow conditions can therefore be calculated from a bed load function, we chose to apply the total bed load (bed material load and bed load with wash load excluded) theory of Ackers and White (1973), because it uses dimensional analysis and uses average stream velocity in preference to shear stress, which

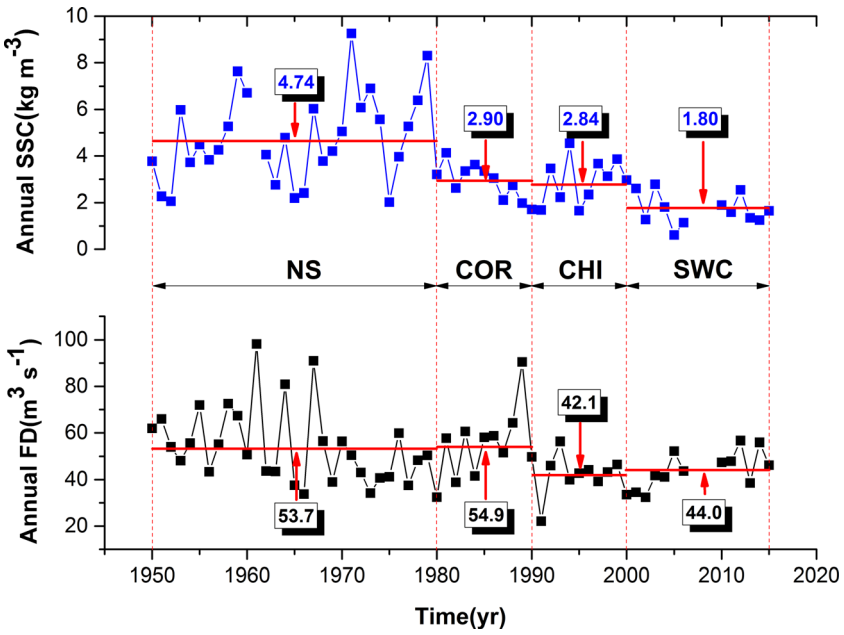

Fig. 4 Annual water and sediment discharge variability from 1950 to 2015 at the Minhe gauge station. The red line represents the average value in each period. Note that the SSC data in 1961 and 2007–2009 period are not available

makes the variables directly related to those available for the Huangshui River.

According to Ackers and White (1973), the dimensionless grain diameter D_{gr} should be determined first as follows:

$$D_{gr} = D_{35}\left[\frac{g(s-1)}{v^2}\right]^{1/3} \tag{2}$$

where s is the mass density of sediment, $s = 1.6$ g cm^{-3}; v is the kinematic viscosity of water; g is gravitational acceleration.

Then, the determination of best-fit coefficients values of n, A, m and C associated with D_{gr}, respectively is as follows:

$$n = 1.00 - .56\log D_{gr}\left(1 < D_{gr} \le 60\right) \tag{3a}$$

$$n = 0\left(D_{gr} > 60\right) \tag{3b}$$

$$A = \frac{0.23}{\sqrt{D_{gr}}} + 0.14\left(1 < D_{gr} \le 60\right) \tag{4a}$$

$$A = 0.17\left(D_{gr} > 60\right) \tag{4b}$$

$$m = \frac{9.66}{D_{gr}} + 0.34\left(1 < D_{gr} \le 60\right) \tag{5a}$$

$$m = 1.5\left(D_{gr} > 60\right) \tag{5b}$$

$$\log C - 2.86\log D_{gr} - \left(\log D_{gr}\right)^2 - 3.53\left(1 < D_{gr} \le 60\right) \tag{6a}$$

$$C = 0.025\left(D_{gr} \le 60\right) \tag{6b}$$

Then, the particle mobility F_{gr} should be calculated as follows:

$$F_{gr} = \frac{v_*^2}{\sqrt{gD_{35}(s-1)}}\left[\frac{V}{\sqrt{32}\log\left(\frac{\alpha d}{D_{35}}\right)}\right]^{1-n} \tag{7a}$$

For coarse sediments ($n = 0$) the expression reduces to the form

$$F_{gr} = \frac{V}{\sqrt{gD_{35}(s-1)}}\frac{1}{\sqrt{32}\log\left(\frac{\alpha d}{D_{35}}\right)} \tag{7b}$$

and for fine sediments ($n = 1$)

$$F_{gr} = \frac{v_*}{\sqrt{gD_{35}(s-1)}} \tag{7c}$$

where v_* is shear velocity; V is mean velocity of flow; $\alpha = 10$; d is flow depth.

At last, transport of transitional sizes of sediment G_{gr} and the sediment flux converted through G_{gr} are calculated as follows:

$$G_{gr} = C\left(\frac{F_{gr}}{A} - 1\right)^m \tag{8}$$

$$G_{gr} = \frac{Xd}{sD_{35}}\left(\frac{v_*}{V}\right)^n \tag{9a}$$

For coarse sediment ($n = 0$)

$$G_{gr} = \frac{Xd}{sD_{35}} \tag{9b}$$

and for fine sediment ($n = 1$)

$$G_{gr} = \frac{Xd}{sD_{35}}\frac{v_*}{V} \tag{9c}$$

Finally, the suspended sediment rating curves based on Eq. (1) were fitted to each of the four data sets mentioned above (Appendix Table 1). A comparison of the curves fitted in

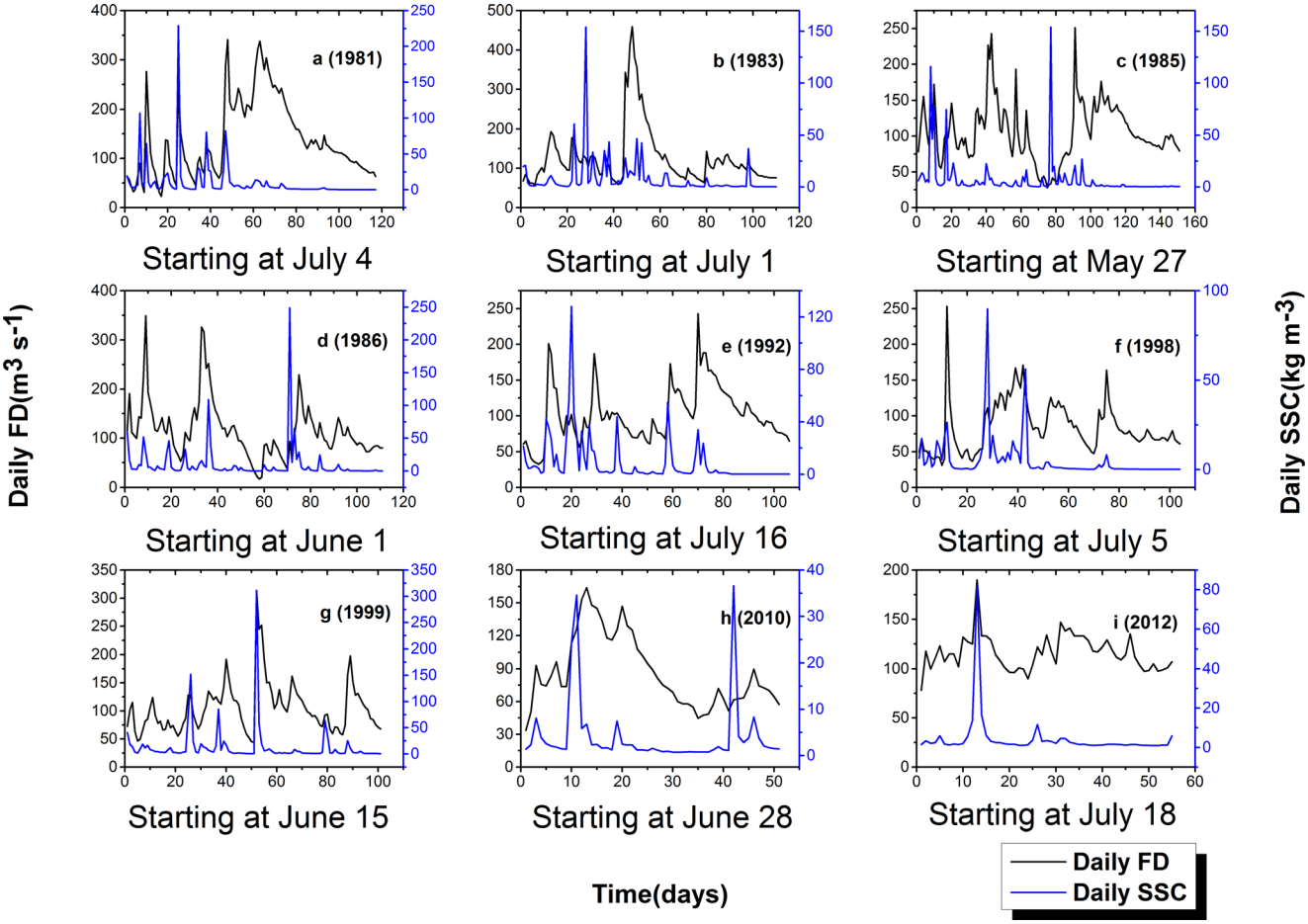

Fig. 5 Hydrographs and SSCs of the nine selected sediment-laden flows. **a**–**d** The four flows in the COR period (1980–1990) and **e**–**g** the three flows in the CHI period (1990–2000) and **h**–**i** the two flows in the SWC period (2000–2015)

different periods provides an indication of the water-sediment characteristics and the transport rate in response to the changes in watershed characteristics due to eco-environmental changes. In addition, the bed load transport dynamics were determined by the results of calculation based on the selected functions. A comparison of the measured and calculated total sediment transport rate was made to validate the application of the selected theory to the Huangshui River.

Results

Temporal variation of the water-sediment relations

As shown in Fig. 4, the annual FD decreased by approximately 21% since 1990 mainly due to the increase of temperature and decrease of precipitation. The annual SSC, however, has experienced an obvious decrease process mainly in response to successive construction and operation of the hydropower structures since 1980. These transverse structures are significantly different from those dams and reservoirs, with few regulation and storage functions for water but can trap most of the upstream incoming coarse-grained bed material, leading to a decrease of nearly 50%. Then, followed by the FD decrease due to climate change since 1990 and the soil and water conservation measures preventing some wash load from delivering into the stream channel since 2000, the SSC in the lower Huangshui River maintained a continuous decreasing trend. Correspondingly, a change in the sediment transport regime occurred, with a decreasing importance of high discharge years.

Sediment transport changes identified through rating curves

Suspended sediment rating curves

The suspended sediment rating curves of four different periods were fitted for the Minhe gauge station on the lower Huangshui River, and our results indicated that the relationship between SSC and FD in the COR period reveals a positive but relatively weak correlation. The correlation coefficient

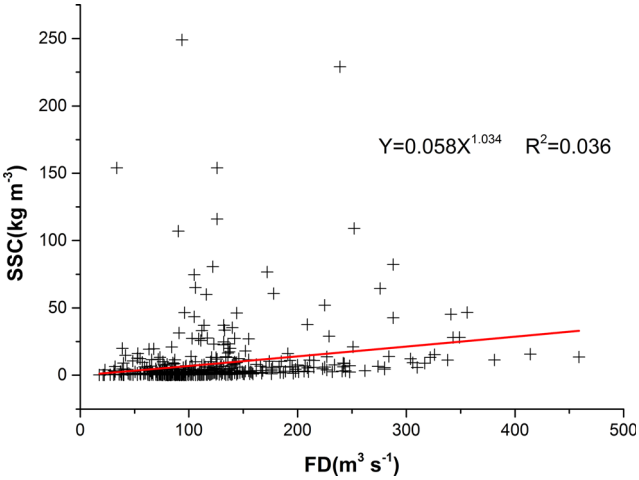

Fig. 6 Suspended sediment rating curve of the COR period (1980–1990) (489 data points)

of the fitting curve shown in Fig. 6 is very low ($R^2 = 0.036$), and even that of NS period is difficult to assess with the scatter in the large number of data points ($N = 993$, plot not shown). However, the rating relationships of the CHI and SWC periods demonstrate a better fit between the related SSC and FD (Figs. 7 and 8), with the R^2 to be 0.425 and 0.547, respectively, indicating that the matching of water-sediment is adjusting to a new equilibrium state under the influence of natural and human activities factors. Physically, we can obviously find that both the FD and SSC were decreased as compared with those of the NS and COR periods, which on the one hand may be attributed to the limit of wash load supply from the watershed, and to the limit of hydraulic carrying capacities to bed materials originating from the stream channel on the other hand. A further comparison of the FD-SSC relationships pre and past 1980 implied that the significant low R^2 value may be related to the frequency of high SSC event-occurrence.

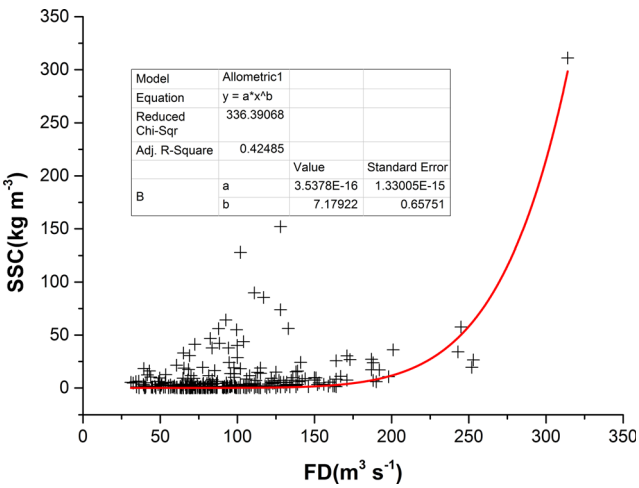

Fig. 7 Suspended sediment rating curve of the CHI period (1990–2000) (311 data points)

As shown in Fig. 6, the number of high SSC points is large, indicating a high occurrence frequency. This stochastic phenomenon, although rare event, is generally related to high hydraulic carrying capacities and the corresponding larger grain size, which cannot be characterized by the power function and even the other suspended sediment rating curves taking different forms proposed by Asselman (2000), leading to a low value of R^2 and the failure of suspended sediment rating curve method to determine the total sediment transport dynamics arbitrarily. To further understand the sediment transport mechanisms, it is necessary to distinguish between fine wash load independent of river flow and coarse bed material components dependent upon flow hydraulics in terms of grain size analysis of available water-sediment samples.

GSDs analysis on suspended sediment samples

Twenty-five suspended sediment data were selected from the measured water-sediment samples including cross-section averaged and point-integrated GSDs during the flood season of 2010–2014 period, with five data each year. According to Einstein (1950), Shen (1971), Partheniades (1977) and Belperio (1979) and the fact that the Huangshui River is located at Chinese Loess Plateau, we define silt and clay (< 0.063 mm in diameter) originating from weathered materials on the gully slopes and delivered into the mainstream channel by heavy rainfall as wash load irrespective of river flow and those sand (0.063–0.125 mm) and sand to grain particles (0.125–1.0 mm) as bed materials suspended from the channel bed by flow turbulence. The GSDs and the instantaneous hydraulic variables are shown in Appendix Table 2.

Our results of GSD analysis demonstrated that a considerable fraction of bed materials (30% on average) occurred in response to high FD-high SSC years of 2010 and 2012, and

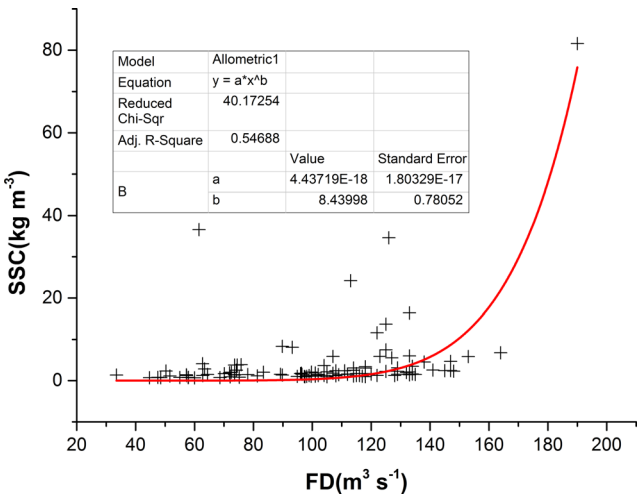

Fig. 8 Suspended sediment rating curve representative approximately of the wash load rating curve of the SWC period (2000–2015) (106 data points)

for annual average conditions, approximately 85% of the suspended sediment components is wash load despite of all flow stages (Fig. 9), indicating further that wash load transport is irrespective of river flow and bed material load transport is hydraulic conditions dominated. In other words, suspended sediment rating curves can only be used to wash load transport for accuracy and the indiscriminant use of wash load and bed material load can therefore lead to ambiguous results.

Bed load transport and the related rating curve

The selected theory has been proven to agree well with several observed rivers with Froude number (F_r) smaller than 0.8 and flume studies (White et al. 1975; Nordin 1977; Yang 1977; Fu and Liu 2017), and here we chose this method to analyze the total bed load transport (wash load excluded) in the lower Huangshui River ($F_r < 0.8$).

To facilitate our calculation and to validate its application in the Huangshui River, the hydraulic and physical variables related are available for 16 specific flow rates of the Huangshui River. As shown in Appendix Table 2, the selected data covers a wide range of flow stages in order to determine the true transport mode with accuracy. The theoretical bed load sediment concentration (SC) calculated by this method was plotted against the related FD to establish the bed load rating curve (Fig. 10). The results demonstrated a better relationship between FD and SC, with R^2 to be 0.877.

Discussion

Interpretation of the suspended sediment rating curve

Our results indicated that wash load should be delineated from the total suspension in the determination and recognization of the true transport mode, and an indirect empirical relationship between FD and fine sediment transport do exist in the form of wash load rating curve, where FD variation is just the reflection of rainfall intensity and duration (Ellison 1945; Wischmeier and Smith 1958; Dragoun 1962; Guy 1964; Yang and Francisco 2005). In other words, heavy rainfall-induced floods and the related severe erosion from the watershed are responsible for the

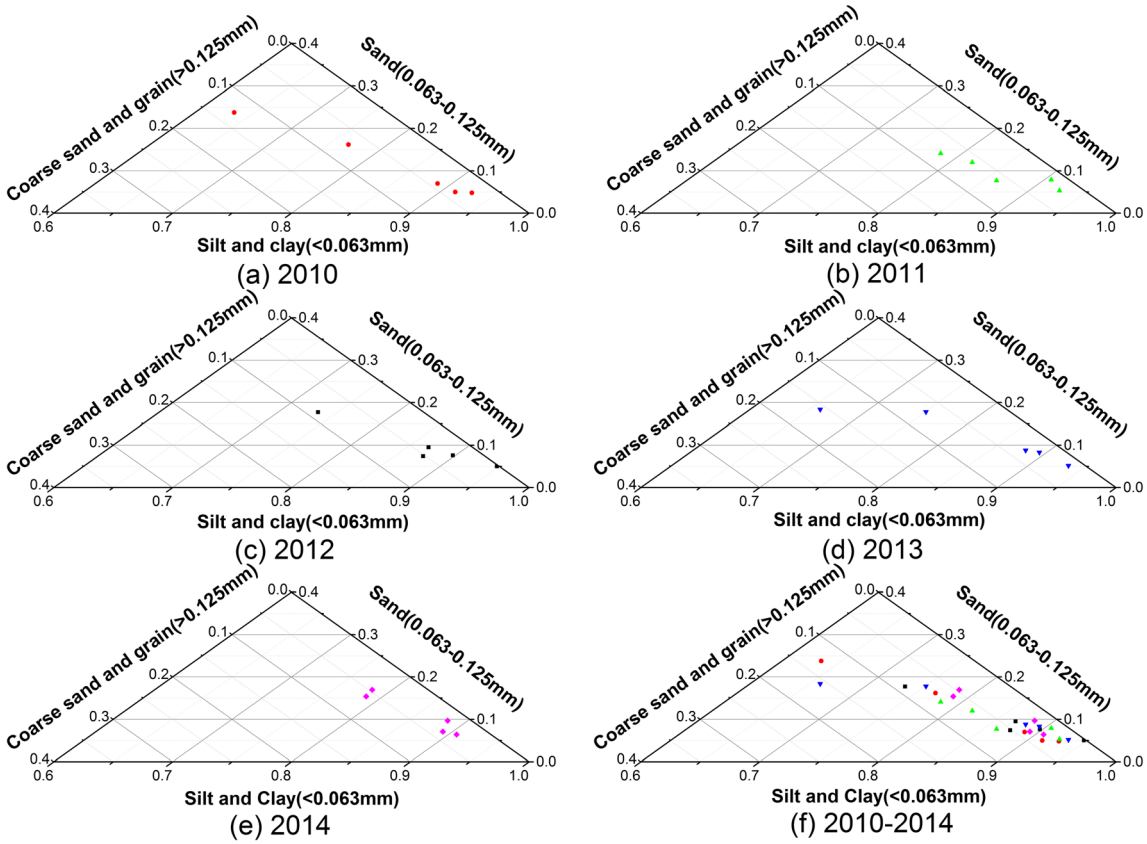

Fig. 9 Grain size analysis of the collected suspended sediment samples under different flow stages in the SWC period (2010–2015). **a** Annual FD = 47.4 $m^3 s^{-1}$, SSC = 1.9 kg m^{-3}. **b** Annual FD = 47.9 $m^3 s^{-1}$, SSC = 1.59 kg m^{-3}. **c** Annual FD = 56.7 $m^3 s^{-1}$, SSC = 2.54 kg m^{-3}. **d** Annual FD = 38.5 $m^3 s^{-1}$, SSC = 1.35 kg m^{-3}. **e** Annual FD = 55.9 $m^3 s^{-1}$, SSC = 1.25 kg m^{-3}. **f** Annual-averaged FD = 49.3 $m^3 s^{-1}$, annual-averaged SSC = 1.72 kg m^{-3} (see detail in Appendix Table 2 for instantaneous hydraulic variables)

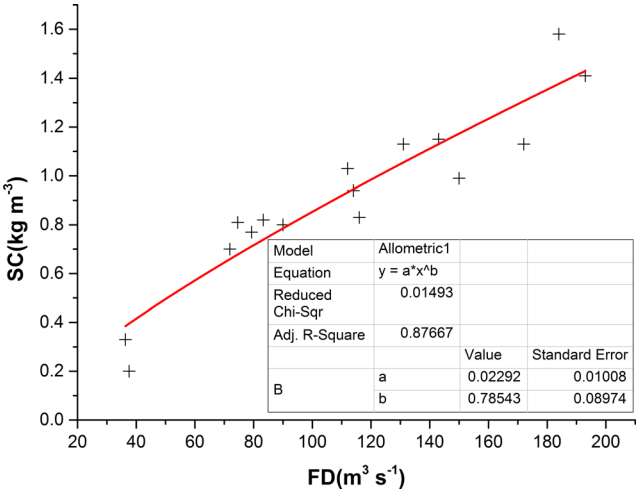

Fig. 10 Bed load rating curve based on 16 measured FDs and theoretically calculated SCs during the SWC period (2010–2015)

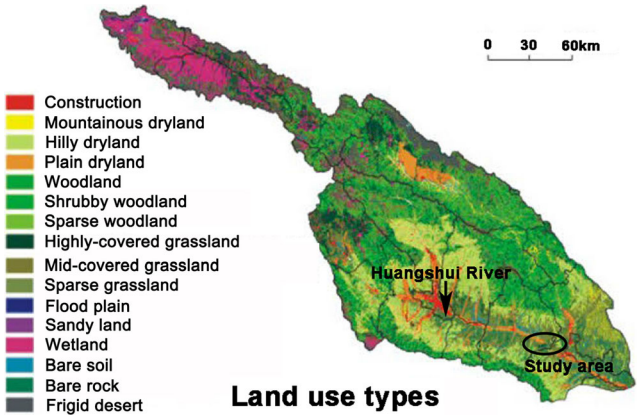

Fig. 11 Plan view of the Huangshui River basin showing different gully erosion grades. The Datong River is the tributary of the Huangshui River (Bai and Yan 2013)

higher river flow and therefore the increase in concentration of wash load. In this sense, wash load rating curves combined with their rating coefficients and exponents are the indicator of the variation of watershed characteristics (Walling 1974; John and Beschta 1983; Sarma 1986; Reid and Dunne 1996; Peters-Kümmerly 1999; Hovius and Lin 2000; Wainwright and Mulligan 2013).

As shown in Figs. 7 and 8, the R^2 increased gradually form 0.425 in the 1990s to 0.547 in the 2000s, indicating significant changes in watershed characteristics mainly due to channel modification and soil and water conservation in the lower Huangshui River. The Huangshui River basin has long been subjected to severe soil erosion and 47.3% of the total drainage area was characterized by soil and water loss by 2000 (Zhao et al. 2008), a rate much higher than the national average level. Therefore, comprehensive ecological management has occurred since 2000 to solve this problem. According to Bai and Yan (2013), nearly 50% of the total area was covered by grassland until 2009 (Fig. 2), and the slope erosion was effectively controlled. Nevertheless, gully erosion was still severe, especially in the reach located within 50 km upstream of the Minhe gauge station (Fig. 11). The lower Huangshui River experienced a net increase of the area of gully erosion of 706.87 km^2 from 2000 to 2009, and the deterioration trend maintained, which is the dominant sediment source of the Huangshui River and even that of the upper Yellow River. Most of the eroded materials delivered into the Huangshui River by rainfall-induced runoff maintain in suspension as wash load, having important effects on the morphology, flood characteristics, and ecology of downstream channels and estuaries.

Although high discharge flood events still played critical roles in transporting sediment, the climate change combined with channel modification as well as comprehensive ecological management regulated and weakened the event-based discharge pattern (e.g., FD peaks and SSC peaks decreased considerably, as shown in Appendix Table 1 and Fig. 5), which ultimately led to the dominance of wash load fractions in the suspended sediment components. Some researchers also suggested that it is reasonable and necessary to exclude extreme sediment transport rates such as bed material load maintaining in suspension by flow turbulence and water-sediment release by reservoirs from populations of sediment-yielding processes to derive a meaningful at-site wash load rating curve and a good rating curve should indicate the sediment production pattern and fluvial erosion power, as well as other basic factors (David et al. 2013). Presumably, if the rating curve in Fig. 8 is further corrected and modified, the rating relationship will be improved with more accuracy. However, the R^2 will not be expected to increase greatly because the variability in the wash load concentration cannot be explained absolutely by variation in FD. Many other factors also control sediment erosion and therefore wash load concentration besides rainfall intensity and duration, such as previous rainfall history, vegetation cover conditions, and antecedent soil conditions (Belperio 1979; Wang et al. 2013). As shown in Fig. 5, erosion is discovered to be the greatest during the first several rainfall-induced floods at the beginning of the wet period, especially of the rainfall occurring over the erodible weathered gully slopes 50 km upstream the Minhe gauge station. The rainfall-induced sediment-laden flows quickly merged into the mainstream of the Huangshui River and flushed rapidly downstream along the mainstream, reaching the Minhe gauge station within a short time due to steep channel gradient (S = 0.0013 for the mainstream channel and 0.035~0.04 for the three tributaries located 500 m upstream) (Ren 2000), with no apparent SSC peak hysteresis. This sediment

erosion and transport process is similar with the Thames River is called flushing effect (Bussi et al. 2016).

Therefore, we define the rating curve shown in Fig. 8 approximately as the wash load rating curve applied to the lower Huangshui River. As several findings regarding the sediment transport in the Yellow River have indicated that the upstream incoming wash load supply has important effects on the water-sediment relations and even the bed load transport in the Inner Mongolia desert reach and middle reach (Yang and Franscisco 2005; Ta, et al. 2015), the wash load rating curve in the form of Fig. 8 is important for such a high sediment yield tributary transporting a large proportion of wash load and contributing a lot to the suspended sediment of the downstream Yellow River.

Explanation of the bed load calculation

Ackers and White's (1973) bed load transport theory we chose to calculate bed load transport is based on correct physical mechanisms and it obey the stream power concept in substance, which is theoretically derived from turbulence theory. As compared with many other theories, however, its derivation also involves many assumptions and generalizations, thus should be improved through application in natural rivers in time. All the variables necessary for calculation we use, although measured, involve approximations to some degree, among which shear velocity $v_* = \sqrt{gdi}$, where the water surface slope $i = 0.0013$ is assumed equivalent to the bed slope S for such a uniform sediment-laden flow (Woo et al. 1988). In addition, although the bed load rating curve (Fig. 10) is based on 16 specific flow rates of the Huangshui River. Which covers a wide range of flow stages occurred under nowadays normal flow conditions, the possibility of extreme high flow events always exists due to the stochastic feature of hydrological phenomenon. Therefore, the accuracy for the total sediment transport rate can certainly be improved. Here, we expect the validation results to determine the application of this theory in the Huangshui River.

Validation of the sediment transport dynamics

Converting the data of wash load and bed load rating curves (Figs. 8 and 10) to transport rate values by multiplying sediment concentration with FD, we established the relationship between sediment transport rate and FD for wash load (q_{sw}) and bed load (q_{sb}), respectively (Figs. 12 and 13). Obviously, the transport rate of the total load should be the sum of the q_{sw} and q_{sb}. Therefore, the transport rate of total sediment (q_s) was plotted against the data values of FD same as those in Fig. 8, as shown in Fig. 14. Then, we used the measured data (daily

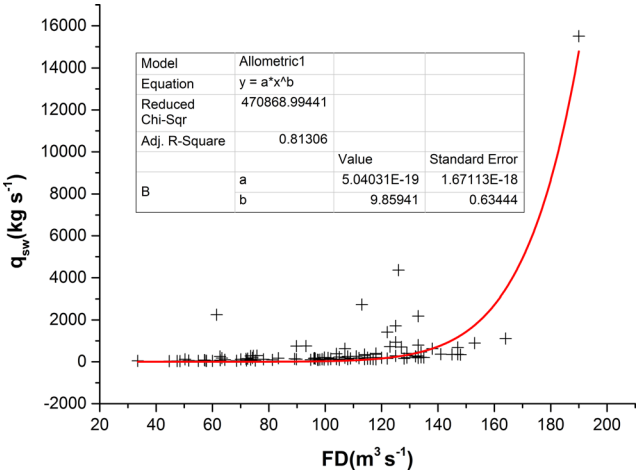

Fig. 12 Plot of wash load transport rate against FD during the SWC period (106 data points)

suspended sediment transport rate) of the same period to valid the theoretically calculated curves (Fig. 15).

As shown in Fig. 15, under the relative higher flow rates (FD = 120~200 m^3 s^{-1}), the calculated values are larger than the simulated values, which is rational because hydraulic factors become dominant and therefore coarse sediment entrainment rate increases, thus, combined with bed materials saltating and rolling on the bed surface, the total sediment transport rate exceeds that of suspended sediment. For annual-averaged flow rates since 2000 (FD = 43.01 m^3 s^{-1}), the estimates of total sediment transport is 3.43×10^7 t, among which the total bed load is 1.40×10^7 t, and the wash load is 2.03×10^7 t. The transport ratio of wash load to total bed load is 1.45:1, indicating that the erosion activities in the watershed and fluvial erosion in the stream channel are nearly equally important in sediment transport process. In the design of the hydropower structures on the lower Huangshui River, the bed load

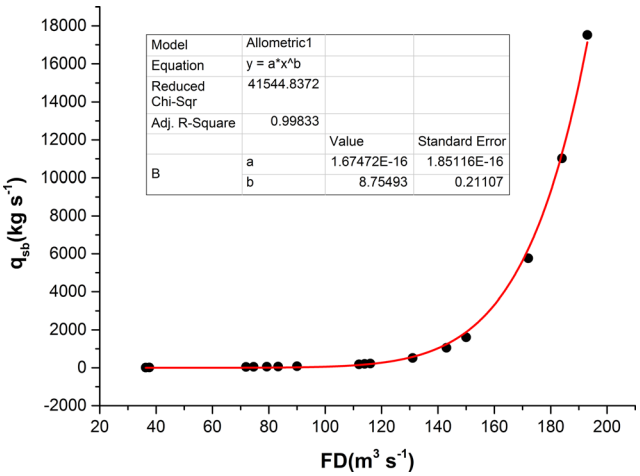

Fig. 13 Plot of bed load transport rate against FD during the SWC period (16 data points)

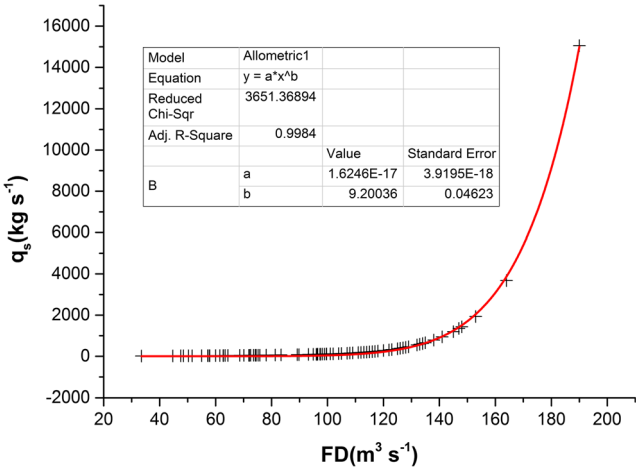

Fig. 14 Plot of total sediment transport rate against FD during the SWC period (106 data points)

has long been estimated through multiplying the conventional suspended sediment load (wash load and suspended bed material load) ($1.8\sim2.4 \times 10^7$ t; Li and Quan 2011) by an empirical coefficient 0.15 based on the analysis of bed material texture. Thus, the total sediment transport is $2.07\sim2.76 \times 10^7$ t, indicating that the order of magnitude of the theoretically calculated values is considered to be correct and the accuracy is satisfying.

In summary, comparison of the measured suspended sediment transport with the theoretically calculated total sediment transport curves can reflect the true transport mode and the inherent sediment dynamics, indicating that the selected method can be applied in the estimate of bed load with more accuracy and the suspended rating relationship between FD and SSC can represent the wash load rating curve under nowadays flow conditions due to comprehensive ecological management in the lower Huangshui River.

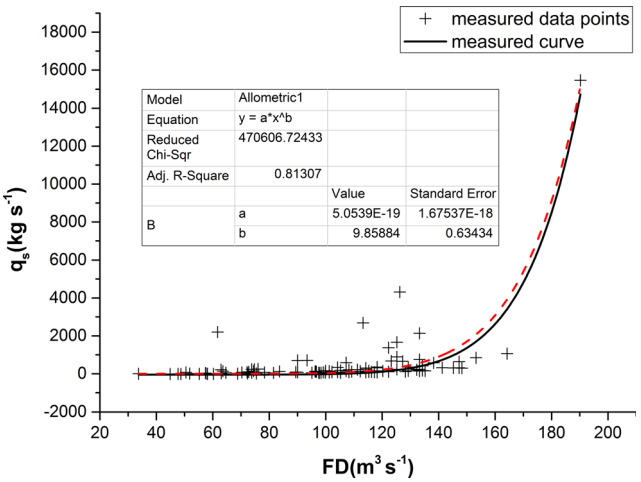

Fig. 15 Comparison of measured suspended sediment transport rate with theoretically calculated sediment rate (106 data points)

Conclusions

Based on the continuous and detailed hydrological data monitored at the Minhe gauge station, the total sediment transport dynamics was studied systematically for the Huangshui River, which is the largest tributary to the upstream reach of the Yellow River and contributes a lot to the suspended sediment load of the upper Yellow River due to the severe soil erosion especially occurred in the lower Hunagshui River basin. According to the water-sediment correlations representing watershed characteristic variability due to natural and man-made factors, the NS, COR, CHI, and SWC periods were subdivided, and 14 sediment-laden flood flows representing wet periods were selected as data preparation. Subsequent results indicated that the sediment transport regime has altered since the 1980s in response to the eco-environmental changes, with SSC decreased by 50% on average compared with the NS period (1950–1980). Wash load and bed material load was distinguished for the first time to recognize and determine the true sediment transport mode under changing watershed characteristics and flow conditions, respectively. A relationship exists between wash load and discharge in terms of wash load rating curve as the indicator of watershed characteristic changes while Ackers and White's (1973) bed load function (with wash load excluded) was validated rational in determining mainstream bed load transport dynamics. The estimate of total sediment transport due to comprehensive ecological management since 2000 (SWC period) is 3.43×10^7 t for the lower Huangshui River, among which the total bed load is 1.40×10^7 t, and the wash load is 2.03×10^7 t. The transport ratio of wash load to total bed load is 1.45:1. The combined use of wash load rating curve and theoretical bed load function is suggested and expected to be applied in determining the true sediment transport mode of the event-based, high sediment yield rivers draining arid zones where erosion activities in the watershed and fluvial erosion in the stream channel are nearly equally important in sediment transport process.

Acknowledgments The authors acknowledge Professor Junsheng Nie from Lanzhou University, China for assistance in creating maps and the Hydrology and Water Resources Bureau of the Upper Yellow River, Yellow River Conservancy Commission of the Ministry of Water Resources for providing the discharge and suspended sediment data. Great thanks to the academic editor and reviewers for their help to improve the article.

Funding information This work was supported by the Natural Science Foundation of China (No. 51269009), the National Basic Research Program of China (No. 2011CB403302), and the West Light Talents Foundation of Chinese Academy of Sciences, 2012 (29Y329971) "Transport Mechanism of coarse sediment in desert watershed in arid zones—a case of Ningxia-Inner Mongolia Reach of Yellow River".

Appendix

Table 1 Characteristics of the selected 14 typical sediment-laden flood events from 1950 to 2015

1950–1980					1980–1990					1990–2000					2000–2015				
Annual FD > 53.7 $m^3 s^{-1}$; SSC > 4.74 kg m^{-3}					Annual FD > 54.9 $m^3 s^{-1}$; SSC > 2.90 kg m^{-3}					Annual FD > 42.1 $m^3 s^{-1}$; SSC > 2.84 kg m^{-3}					Annual FD > 44.0 $m^3 s^{-1}$; SSC > 1.80 kg m^{-3}				
Year	Date	FD Peak	Date	SSC Peak	Year	Date	FD Peak	Date	SSC Peak	Year	Date	FD Peak	Date	SSC Peak	Year	Date	FD Peak	Date	SSC Peak
1958	24 Jun.	428	8 Aug.	232	1981	20 Aug.	341	28 Jul.	229	1992	23 Sept.	243	4 Aug.	128	2010	10 Jul.	164	8 Aug.	36.6
1959	15 Jul.	502	27 Jul.	236	1983	17 Aug.	459	28 Jul.	154	1998	16 Jul.	253	1 Aug.	89.8	2012	30 Jul.	190	30 Jul.	81.6
1964	1 Jun.	319	19 Aug.	133	1985	25 Aug.	251	11 Aug.	154	1999	5 Aug.	314	5 Aug.	311					
1967	3 Aug.	460	6 Aug.	210	1986	9 Jun.	349	10 Aug.	249										
1970	18 Aug.	475	7 Aug.	374															

Table 2 Suspended sediment grain size distributions (GSDs) and main flow variables related to total bed load calculation

Year	Time	Fine	Medium	Coarse	Suspended sediment grain size distribution (%)										Total bed load calculation					
		(mm)			(mm)										FD	D_{35}	v	dx	v_*	SC
		< 0.063	0.063–0.125	> 0.125	0.002	0.004	0.008	0.016	0.031	0.063	0.125	0.25	0.50	1.0	(m^3/s)	(mm)	(m/s)	(m)		(kg/m^3)
2010[a]	6.30	91.3	5	3.7	8.7	19.4	37.3	60.0	79.2	91.3	96.3	98.5	99.9	100	83.3	0.5	1.74	1.19	0.123	0.82
	7.7	63.3	23.8	12.9*	5.0	9.0	14.9	22.5	36.2	63.3	87.1	96.3	99.7	100	74.6		1.7	1.11	0.119	0.81
	7.9	76.7	16.2	7.1	6.8	13.0	22.1	33.9	51.0	76.7	92.9	96.7	99.7	100	184		2.62	1.71	0.148	1.58
	7.16	92.8	4.8	2.4	16.8	32.8	50.9	68.6	82.5	92.8	97.6	99.7	100		112		2.03	1.37	0.132	1.03
	8.12	88.8	7	4.2	8.7	18.9	35.0	55.8	74.7	88.8	95.8	98.9	100		131		2.21	1.44	0.135	1.13
2011[a]	7.6	81.9	12	6.1	6.9	14.9	27.6	44.8	63.1	81.9	93.9	98.9	100			0.5				
	8.14	92.6	5.3	2.1	13.2	26.4	44.1	64.5	81.1	92.6	97.9	99.6	100		36.3		1.16	0.88	0.106	0.33
	8.15	86.1	7.7	6.2*	7.1	15.5	29.6	50.7	71.5	86.1	93.8	98.3	100		116		2.04	1.54	0.140	0.83
	8.18	78.2	14.1	7.7	7.2	15.3	27.4	42.8	59.3	78.2	92.3	98.6	100		150		2.31	1.76	0.150	0.99
	9.7	90.6	7.9	1.5	13.0	24.8	38.9	55.0	72.7	90.6	98.5	99.8	100		143		2.32	1.67	0.146	1.15
2012[a]	7.19	89.8	7.6	2.6	8.6	17.8	31.8	51.1	71.6	89.8	97.4	99.7	100		114	0.5	2.1	1.59	0.142	0.94
	7.30	94.8	5	0.2*	16.8	31.2	48.3	66.7	82.5	94.8	99.8	100			193		2.7	2	0.160	1.41

Table 2 (continued)

Year	Time	Fine	Medium	Coarse	Suspended sediment grain size distribution (%)										Total bed load calculation					
		(mm)			(mm)										FD	D_{35}	v	dx	v_*	SC
		< 0.063	0.063–0.125	> 0.125	0.002	0.004	0.008	0.016	0.031	0.063	0.125	0.25	0.50	1.0	(m^3/s)	(mm)	(m/s)	(m)		(kg/m^3)
	8.12	87.4	7.4	5.2	8.9	19.1	34.6	54.6	73.0	87.4	94.8	97.9	99.6	100						
	8.17	73.4	17.7	8.9	6.8	13.3	22.6	35.0	51.1	73.4	91.1	98.7	100		172		2.51	1.9	0.156	1.13
	9.10	86.8	9.5	3.7	9.5	18.2	30.5	47.3	67.0	86.8	96.3	99.2	100							
2013[b]	6.26	75.1	17.8	7.1	7.1	13.8	23.2	36.1	51.9	75.1	92.9	97.8	100							
	7.19	65.9	18.4	15.7*	5.8	11.7	20.6	32.5	46.8	65.9	84.3	94.8	99.8	100	71.9		1.72	1.27	0.127	0.7
	7.27	88.0	8.8	3.2	10.3	20.7	35.3	53.5	71.5	88.0	96.8	99.9	100							
	8.17	93.4	5.2	1.4	13.4	26.7	44.4	64.9	81.9	93.4	98.6	100								
	9.11	89.4	8.3	2.3	8.3	17.4	31.3	50.6	70.9	89.4	97.7	99.8	100							
2014[b]	6.3	88.3	9.7	2*	9.6	19.0	31.8	48.5	68.4	88.3	98.0	99.7	100		37.6	0.5	1.12	1.04	0.115	0.2
	6.26	78.3	17	4.7	4.6	9.1	18.7	35.3	53.9	78.3	95.3	99.5	100		90		1.89	1.46	0.136	0.8
	7.31	89.2	7.1	3.7	11.5	23.2	39.0	57.7	75.0	89.2	96.3	98.9	100							
	8.26	78.6	15.4	6	4.5	9.4	19.5	36.5	56.2	78.6	94.0	100								
	10.8	90.7	6.4	2.9	12.2	24.0	39.7	58.3	76.0	90.7	97.1	99.5	100		79.3		1.77	1.38	0.133	0.77

[a] The samples was collected on 14:00 pm

[b] The samples was collected on 8:00 am

*Represents point-integrated sample

References

Ackers P, White WR (1973) Sediment transport: new approach and analysis. J Hydraul Div ASCE 99:2041–2060

Asselman NEM (2000) Fitting and interpretation of sediment rating curves. J Hydrol 234(3–4):228–248. https://doi.org/10.1016/S0022-1694(00)00253-5

Bai XX, Yan CZ (2013). Effects of eco-environmental construction projects on soil and water loss in Huangshui River basin. Bull Soil Water Conserv 33(3): 217–305. (in Chinese)

Belperio AP (1979) The combined use of wash load and bed material load rating curves for the calculation of total load: an example from the BURDEKIN River, Australia. Catena 6:317–329

Bishop AA, Simons DB, Richardson EV (1965) Total bed-material transport. J Hydraul Div ASCE 91:175

Blench T (1969) Mobile-bed fluviology: a regime theory treatment of canals and rivers for engineers and hydrologist. The University of Alberta Press, Edmonton

Burbank DW, Anderson RS (2013) Tectonic geomorphology, second edition. Environ Eng Geosci 19(2):198–200

Colby BR (1964) Practical computations of bed material discharge. J Hydraul Div ASCE 90:217

Dai et al., (2006). Climate change and its effect on the Huangshui watershed. Qinghai Huanjing, 16 (3): 99–101. (in Chinese)

David T, Soong et al (2013) Preliminary analysis of suspended sediment rating curves for the KALAMAZOO River and its tributaries from Marshall to Kalamazoo, Michigan [microform]

Dinehart RL (1998) Sediment transport at gaging stations near Mount St. Helens, Washington, 1980–90, data collection and analysis. Professional Paper

Dragoun FJ (1962) Rainfall energy as related to sediment yield. J Geophys Res 67:1495–1501

Einstein HA (1950) The bed load function for sediment transport in open channel flows. U. S. Dept. of Agric. Soil conservation servie, Technical report No. 1026

Ellison WD (1945) Some effects of raindrops and furface flow on soil erosion and infiltration. Trans Am Geophys Union 26:415–429

Fu HL, Liu XJ (2017) Research on the phenomenon of Chinese residents' spiritual contagion for the reuse of recycled water based on SC-IAT. Water 9(11):846

Bussi G et al (2016) Seasonal and interannual changes in sediment transport indentified through sediment rating curves. J Hydrol Eng 06016016:1–7

Guy HP (1964) An analysis of some strom-period variables affecting stream sediment transport. Geol Surv Prof Pap 462E

Hovius N, Lin JC (2000) Supply and removal of sediment in a landslide-dominated mountain belt: Central Range, Taiwan. J Geol 108(1): 73–89

John VS, Beschta RL (1983) Supply-based models of suspended sediment transport in streams. Water Resour Res 19(3):768–778

Lenzi MA, Marchi L (2000) Suspended sediment load during floods in a small stream of the Dolomites (northeastern Italy). Catena 39(4): 267–282

Leopold L (1968) Hydrology for urban land use planning: a guidebook on the hydrologic effects of urban land use. 554

Li YL, Quan XZ (2011) Analysis on characteristics of the Minhe gauge station on the Huangshui River. Mod Agric Sci Technol (21):2. (in Chinese)

Meade RH, Yuzyk TR, Day TJ (2010) Movement and storage of sediment in rivers of the United States and Canada

Meyer-Peter E, Favre H, Einstein A (1934) Neuere versuchsresultate über den geschiebertrieb. Schweizerische Bauzeitung 103

Meyer-Peter E, Müller R (1948) Formula for bedload transport. International association of hydraulic. Research 2nd meeting, Stockholm, pp 39

Milliman JD, Meade RH (1983) World-wide delivery of river sediment to the oceans. J Geol 91(1):1–21

Milliman JD, Syvitsky J (1992) Geomorphic/tectonic control of sediment discharge to the ocean: the importance of small mountainous rivers. J Geol 100:525–544

Murray HD, Basil G, Trustrum NA (2000) Erosion thresholds and suspended sediment yields, Waipaoa River basin, New Zealand. Water Resour Res 36(4):1129–1142

Ren L (2000) Analyisi on the rainstorm-induced floods in 1998 from the Huanghsui watershed. Gansu Water Conservancy and Hydropower. Technology 3. (in Chinese)

Nordin CF Jr (1977) Discussion in proceeding paper 12103 by C. T. Yang and J. B. Stall. J Hydraul Div ASCE 103:209–211

Partheniades E (1977) Unified view of wash load and bed material load. J Hydraul Div ASCE 103:1037–1057

Peters-Kümmerly BE (1999) Untersuchungen über Zusammensetzung und Transport von Schwebstoffen in einigen Schweizer Flüssen. Geograph Helv 28(3):137–151

Reid LM, Dunne T (1996) Rapid evaluation of sediment budgets. Catena Verlag, Reiskirchen

Rubin DM, Topping DJ (2001) Quantifying the relative importance of flow regulation and grain size regulation of suspended sediment transport alpha and tracking changes in grain size of bed sediment beta. Water Resour Res 37(1):133–146

Sarma JN (1986) Sediment transport in the Burhi Dihing River, India. 199–215

Shen HW (1971) Wash load and bed load. In: Shen HW (ed) River mechanics. Fort Collins, Colorado, pp 11.1–11. 30

Shen HW, Hung CS (1972) An engineering approach to total bed material load by regression analysis. In: Shen HW (ed) Proceedings, sedimentation symposium, Berkeley, California, 14

Shields A (1936) Application of the theory of similarity and turbulence research to the bedload movement. In: Saleh Q (ed) Vers. Wasserbau Scbiffbau, 26th. Mitt. Preuss, Berlin

Syvitski JP, Morehead MD, Bahr DB, Mulder T (2000) Estimating fluvial sediment transport: the rating parameters. Water Resour Res 36(9): 2747–2760

Ta W, Wang H, Jia X (2015) Suspended sediment transport response to upstream wash-load supply in the sand-bed reach of the Upper Yellow River, China. J Hydrol 528:562–570

Topping DJ, Rubin DM, Vierra LE (2000) Colorado River sediment transport: 1. Natural sediment supply limitation and the influence of Glen Canyon Dam. Water Resour Res 36(2):515–542

Trimble SW (1997) Contribution of stream channel erosion to sediment yield from an urbanizing watershed. Science 278(5342):1442–1444

Trimble SW (1999) Decreased rates of alluvial sediment storage in the Coon Creek Basin, Wisconsin, 1975-93. Science 285(5431):1244–1246

Wainwright J, Mulligan M (2013) 22. Soil Erosion and Conservation. John Wiley & Sons, Ltd, pp. 365–378

Walling DE (1974) Suspended sediment and solute yieles from a small catchment piror to urbanization. In: Walling DE (ed) Fluvial processes in instrumented watersheds. Institute of British Geographers Special Publication, Gregory, K, J., pp. 169–192

Wang J, Ishidaira H, Sun W, Ning S (2013) Development and interpretation of new sediment rating curve considering the effect of vegetation cover for Asian basins. Sci World J 2013:1–9. https://doi.org/10.1155/2013/154375

Wang J, Hiroshi I, Ning S, Khujanazarov T, Yin G, Guo L (2016) Attribution analyses of impacts of environmental changes on streamflow and sediment load in a mountainous basin, Vietnam. Forests 7(2):30

Wang XL, Tang HB (2012) Viewing achievements of ecological building in Huangshui watershed from silt-discharge variation of Ledu Hydrometric Station. Soil Water Conserv China (8):3. (in Chinese)

Wang Y, Ren ME, Syvitski JPM (1998) Sediment transport and terrigenous flux 10

Warrick JA, Rubin DM (2007) Suspended-sediment rating curve response to urbanization and wildfire, Santa Ana River, California. J Geophys Res Atmos 112(F2)

White WR, Milli H, Crabbe AD (1975) Sediment transport theories: a review. Proc Inst Civ Eng 59:265–292

Williams GP (1989) Sediment concentration versus water discharge during single hydrologic events in rivers. J Hydrol 111(1–4):89–106

Wischmeier WH, Smith DD (1958) Rainfall energy and its relationship to soil loss. Tran Am Geophys Union 39:285–291

Woo HS, Julien PY, Richardson EV (1988) Suspension of large concentration of sands. J Hydraul Eng 114:888–898

Yang (1977) The movement of sediment in rivers. Geophys Surv 3:39–68

Yang CT (1973) Incipient motion and sediment tranport. J Hydraul Div ASCE 99(10):1679–1704

Yang CT, Franscisco JM (2005) Wash load and bed-material load transport in the Yellow River. J Hydraul Eng 131:413–418

Yang SL et al (2005) Impact of dams on Yangtze River sediment supply to the sea and delta intertidal wetland response. J Geophys Res Earth Surf 110(F3):247–275

Zhao CC, Dong X, Xin WR, Zhang FC, Yang X (2008) Analysis of factors of soil erosion and some ways of rehabilitation in Huangshui River of Qinghai Province. Res Soil Water Conserv 15: 200–201 (in Chinese)